Supplementary Information (SI) for Inorganic Chemistry Frontiers.
This journal is © the Partner Organisations 2026

Supporting Information

Self-assembly of a high-nuclearity fullerene-like heteropolyoxometalate cage

Shuangxue Wu,[a] Chunyi Sun,[a] Xinlong Wang,*[a] Kuizhan Shao,[a] Chao Qin,*[a] and Zhongmin Su[b]

[a]Key Laboratory of Polyoxometalate and Reticular Material Chemistry of Ministry of Education, Northeast Normal University Changchun, Jilin, 130024 (China).

[b]Key Laboratory of Advanced Materials of Tropical Island Resources, Hainan University Haikou, Hainan, 570228 (China).

*Corresponding Author(s): wangxl824@nenu.edu.cn; qinc703@nenu.edu.cn

Experimental Procedures

Crystal data collection and refinements

Single-crystal X-ray diffraction data for the **$Mo_{24}V_{30}P_{48}$** were recorded using a Germany Bruker D8 VENTURE diffractometer with graphite-monochromated Cu Kα radiation (λ = 1.5406 nm) at 293 K. SADABS software was used for multiscan absorption corrections.[1] The crystal structures were solved via the direct method and refined using full-matrix methods against F^2 (diffracted intensity) from the SHELXTL package and Olex2 software.[2] Anisotropic refinement was performed for all non-hydrogen atoms. The restrained DFIX, SIMU, ISOR instructions were used to make the structures more reasonable. The solvent molecules and counterions in **$Mo_{24}V_{30}P_{48}$** are disordered, hindering the modeling of the crystal structure. Therefore, all guest molecules and counterions in **$Mo_{24}V_{30}P_{48}$** were removed using the SQUEEZE option of PLATON. The specific crystallographic data and structure refinement results of the **$Mo_{24}V_{30}P_{48}$** are shown in Table S1. Crystallographic data from **$Mo_{24}V_{30}P_{48}$** was delivered to the Cambridge Crystallographic Data Centre (CCDC) and assigned No. 2505634

Materials and methods

All solid materials, commercial reagents and solvents were used without further purification. $VOSO_4 \cdot xH_2O$, $Na_2MoO_4 \cdot 4H_2O$, phenylphosphoric acid, and $CH_3COONa \cdot 4H_2O$ were purchased from Aladdin commercial companies. Acetonitrile (MeCN), methanol (MeOH), propionic acid, and N, N-Dimethylformamide (DMF) were obtained from Tianjin Fuyu Fine Chemical Co., Ltd. Powder X-ray diffraction (PXRD) tests were carried out on a Smartlab diffractometer radiating through Cu Kα (λ = 0.15418 nm) at a rate of 10° min^{-1} within 5°–50°. Infrared (IR) spectra were recorded on a NICOLET iS50 FT/IR spectrophotometer and the compounds were prepared as KBr pellets method in the range of 4000–400 cm^{-1}. Ultraviolet-visible (UV/vis) absorption spectra were measured on a Cary-7000 spectrometer, over the wavelength range of 200–800 nm. Thermogravimetric analysis (TGA) of **$Mo_{24}V_{30}P_{48}$** was conducted on a DTG-60H analyzer under a nitrogen atmosphere, with heating from room temperature to 800 °C at a rate of 10 °C min^{-1}. The morphology and elemental distribution of **$Mo_{24}V_{30}P_{48}$** were characterized by scanning electron microscopy (SEM; Hitachi SU-70). X-ray photoelectron spectroscopy (XPS) experiments were performed on an XPS system (Thermo-Fisher, ESCLAB 250, USA) to analyze the 3d and 2p orbital energy spectra of Mo and V in **$Mo_{24}V_{30}P_{48}$**. The ESI-MS spectra were obtained using a high-resolution mass spectrometer (model Thermo Scientific Q Exactive) from Thermo Fisher Scientific. In the catalytic oxidation experiment of phenol, the reaction progress of the substrate was monitored using liquid chromatography (LC), and the products were qualitatively identified via ^{1}HNMR.

Results and Discussion

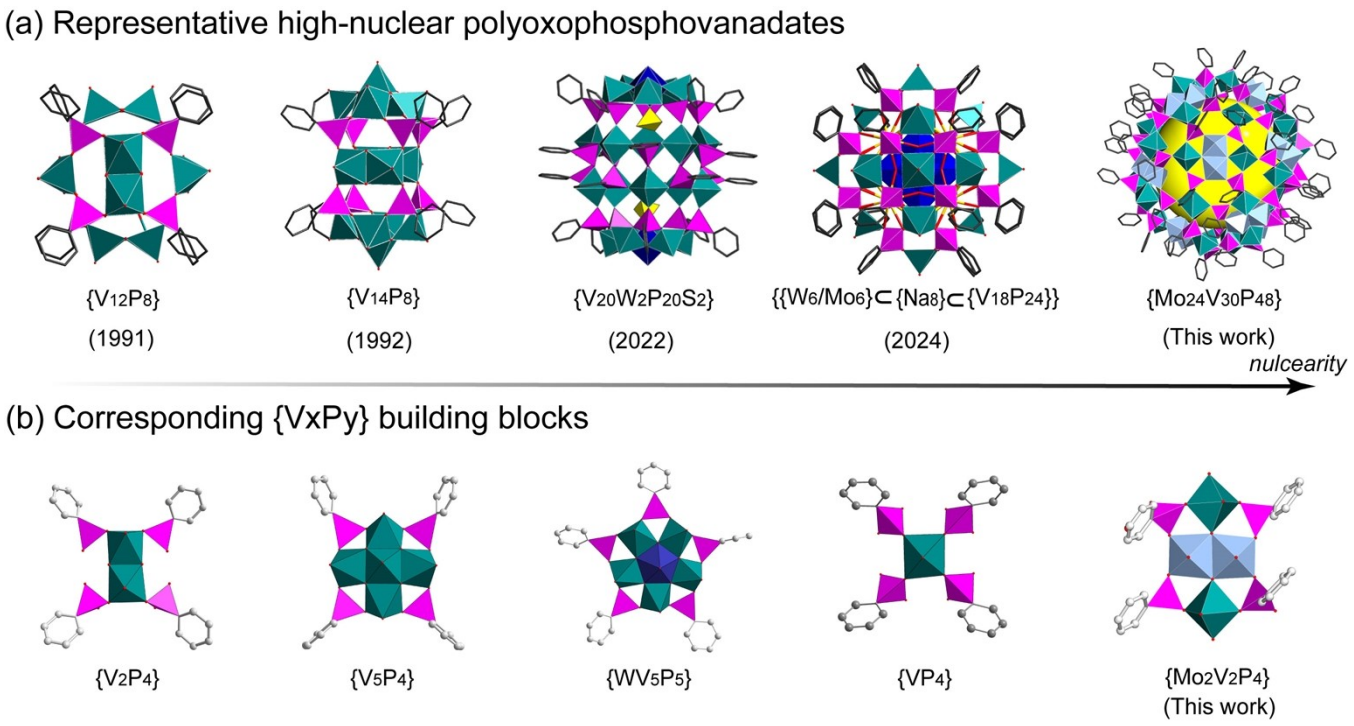

Figure S1. Currently reported high-nuclearity polyoxovanadophosphates and the corresponding {VxPy} building blocks

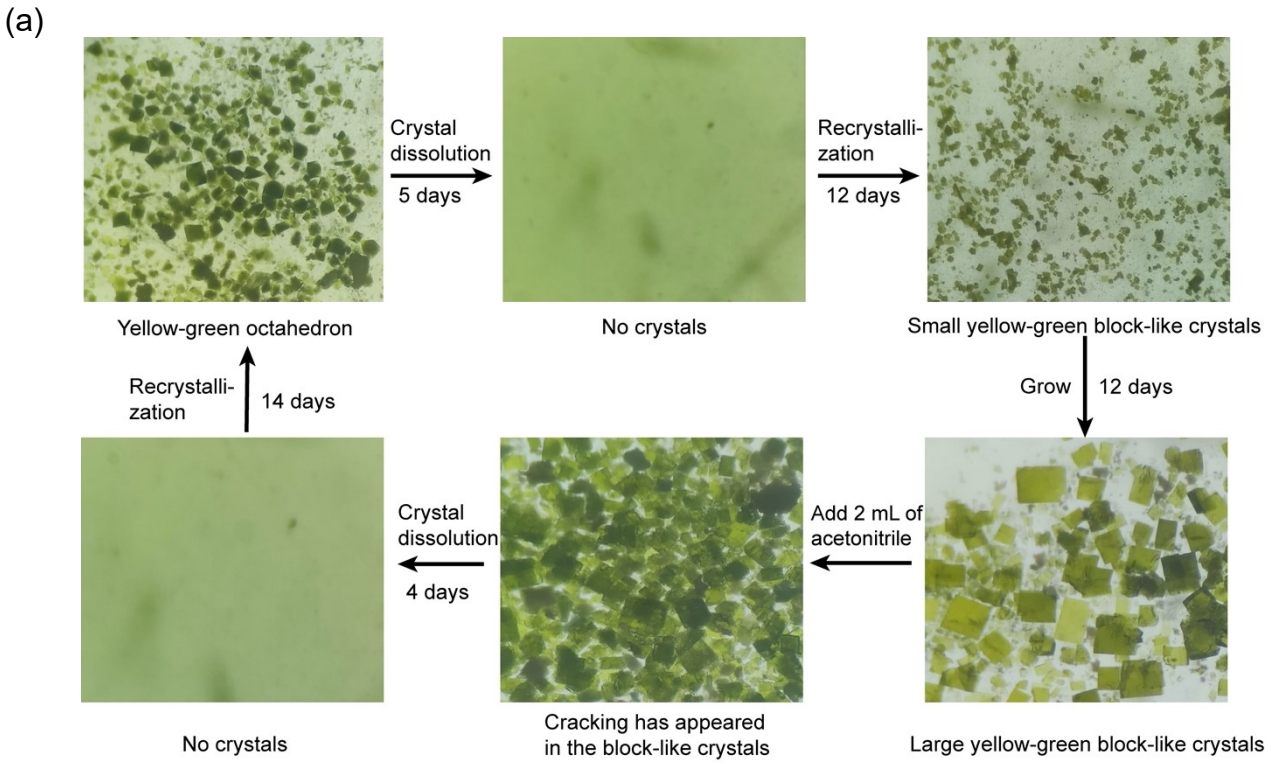

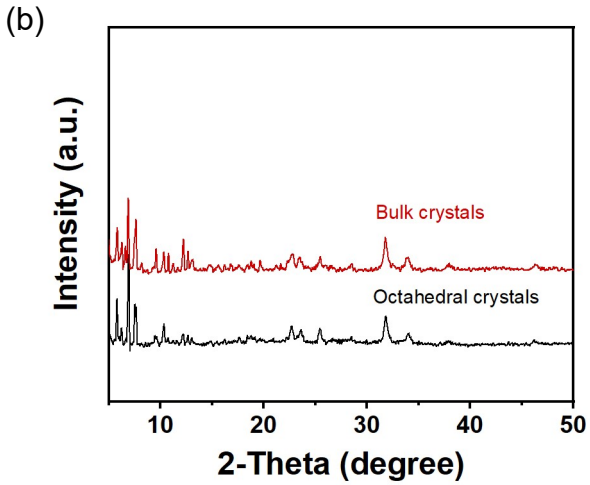

Figure S2. (a) Acetonitrile regulates the crystal morphology of **$Mo_{24}V_{30}P_{48}$**. (b) Powder X-ray diffraction analysis of **$Mo_{24}V_{30}P_{48}$** block crystals and octahedral crystals

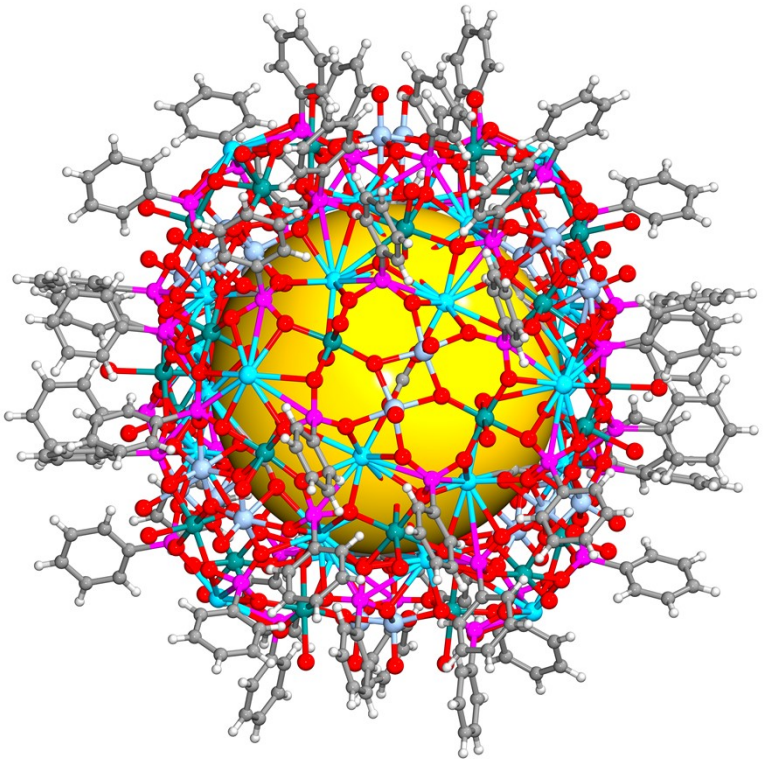

Figure S3. The ball-and-stick model of **$Mo_{24}V_{30}P_{48}$**. Color code: red, O; pink, P; green, V; sky blue, Mo; dark gray, light blue, Na; C; light gray, H

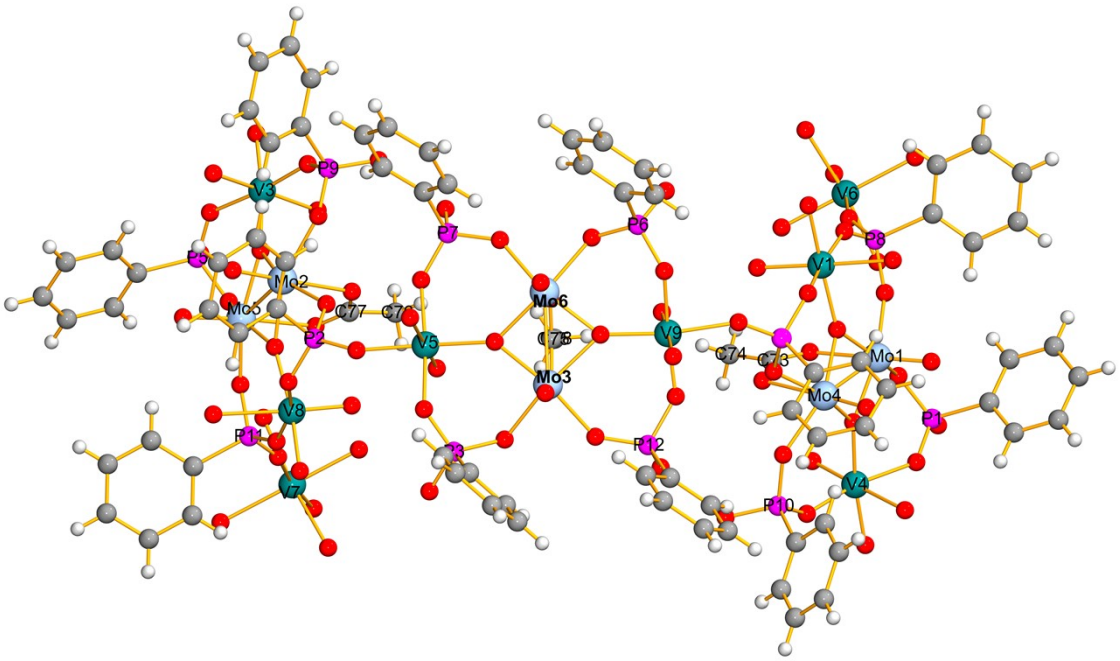

Figure S4. The asymmetric unit of $Mo_{24}V_{30}P_{48}$. Color code: red, O; pink, P; green, V; sky blue, Mo; dark gray, C; light gray, H

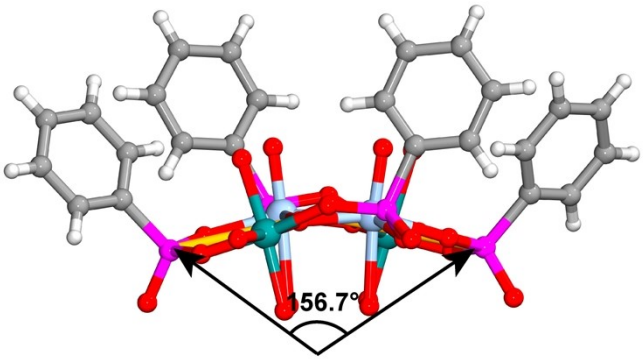

Figure S5. Bending angle of the $\{Mo_2V_2P_4\}$ building block

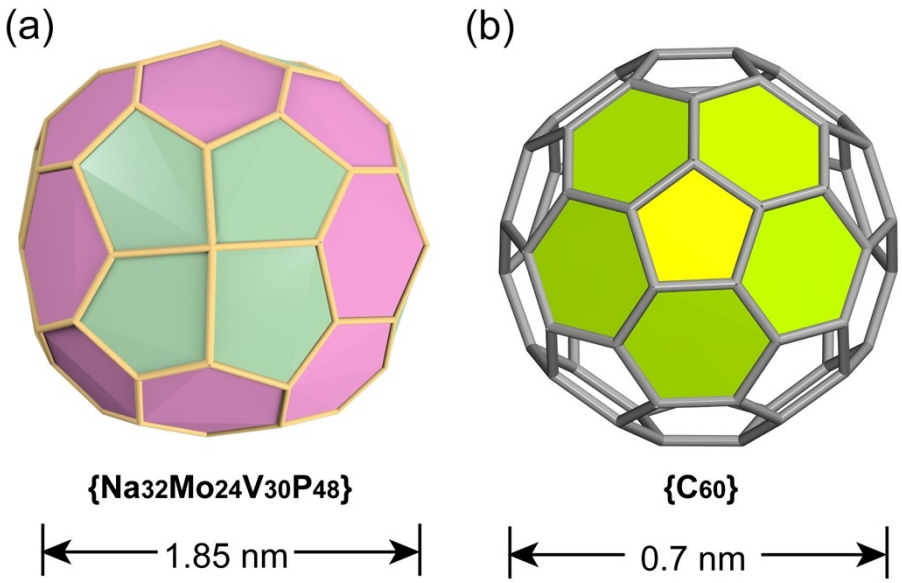

Figure S6. (a) and (b) the polyhedral models of the $\mathbf{Mo_{24}V_{30}P_{48}}$ and C_{60}, respectively.

Table S1. Crystallographic date for $\mathbf{Mo_{24}V_{30}P_{48}}$

Compound	$\mathbf{Mo_{24}V_{30}P_{48}}$
Empirical formula	$C_{312}H_{276}Mo_{24}Na_{32}O_{276}P_{48}V_{30}$
Formula weight	14494.31
Temperature/K	293(2)
Crystal system	tetragonal
Space group	*P4/n*
a/Å	30.0146(14)
b/Å	30.0146(14)
c/Å	37.225(5)
α/°	90
β/°	90
γ/°	90
Volume/Å^3	33535(6)
Z	2
ρcalcg/cm^3	1.435
F (000)	14252.0
Reflections collected	56689
Independent reflections	13129
*R*int	0.0813
Goodness-of-fit on F^2	1.057
Final *R* indexes [I>=2σ (I)]	R_1 = 0.1456, wR_2 = 0.3654
Final *R* indexes [all data]	R_1 = 0.2005, wR_2 = 0.4173

$R_1 = ||F_o| - |F_c||/|F_o|$, $wR_2 = [w(F_o^2 - F_c^2)^2/w(F_o^2)^2]^{1/2}$

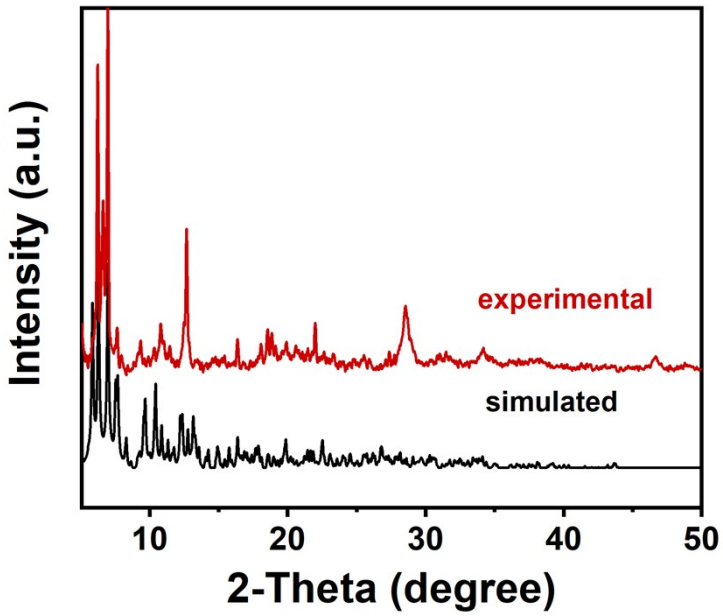

Figure S7. Experimental and simulated powder X-ray diffraction patterns for $Mo_{24}V_{30}P_{48}$.

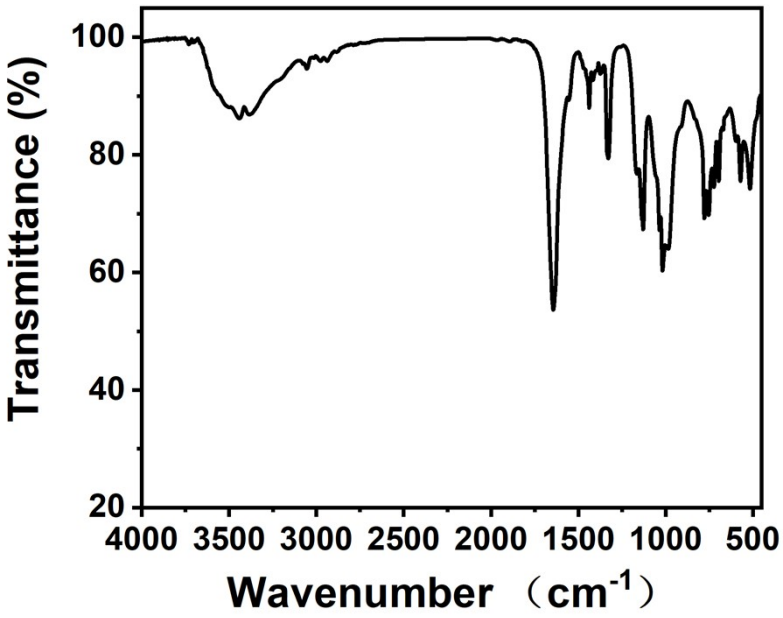

Figure S8. Fourier transform infrared (FTIR) spectra of $Mo_{24}V_{30}P_{48}$.

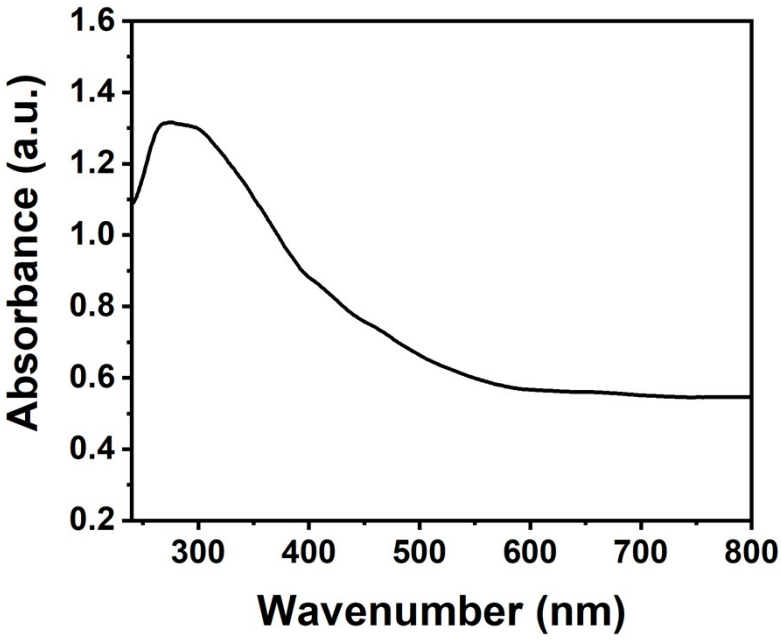

Figure S9. UV-Vis absorption spectroscopy of **$Mo_{24}V_{30}P_{48}$.**

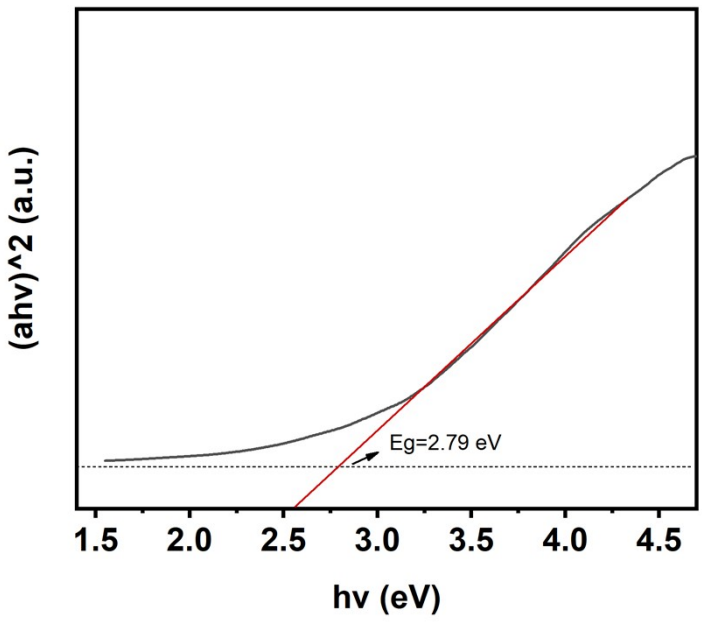

Figure S10. Band structure diagram for **$Mo_{24}V_{30}P_{48}$.**

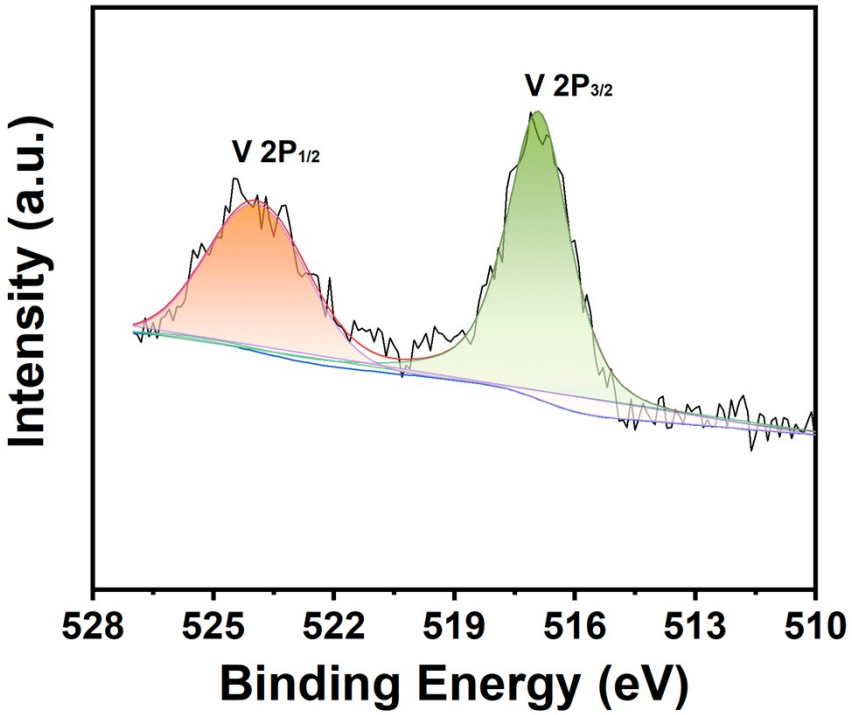

Figure S11. XPS spectra of $\mathbf{Mo_{24}V_{30}P_{48}}$ for V $2p_{3/2}$ and V $2p_{1/2}$

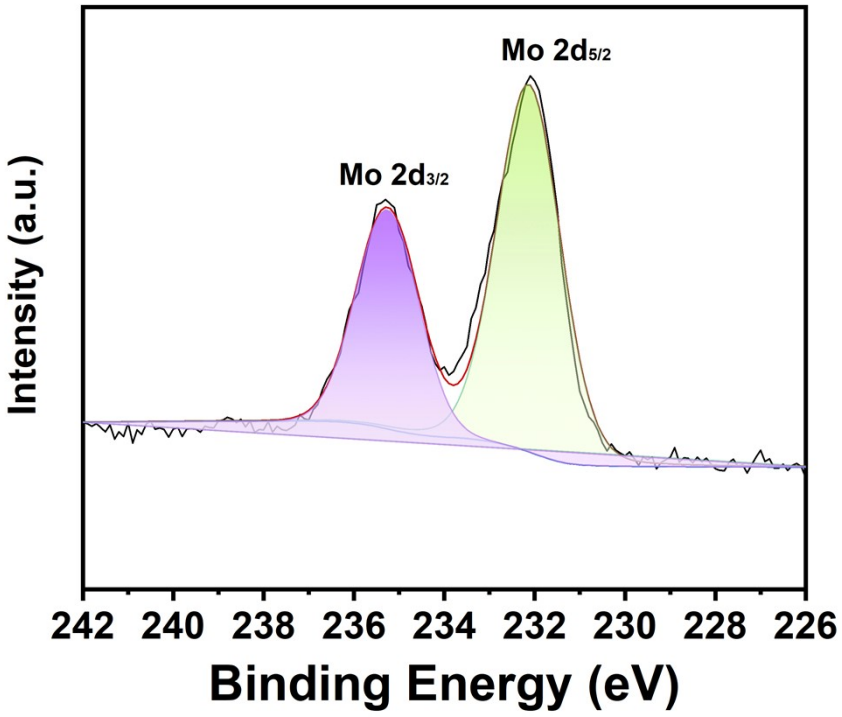

Figure S12. XPS spectra of $\mathbf{Mo_{24}V_{30}P_{48}}$ for Mo $2d_{5/2}$ and Mo $2d_{3/2}$

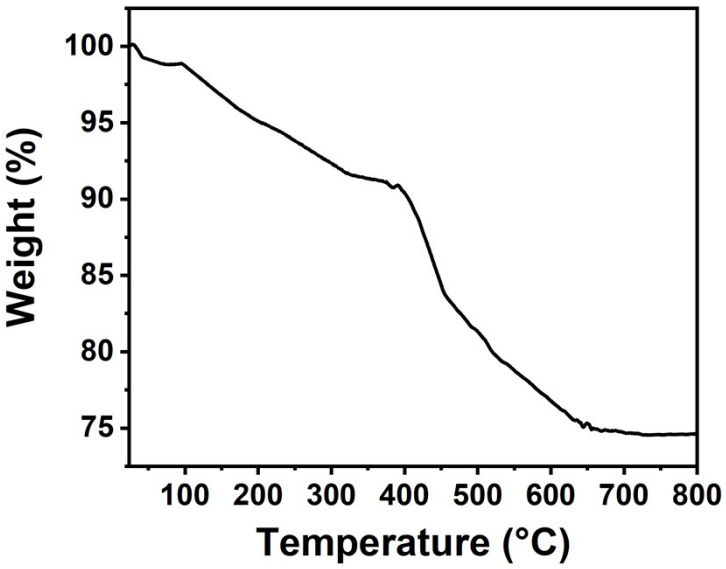

Figure S13. Thermogravimetric analytical traces of **$Mo_{24}V_{30}P_{48}$**.

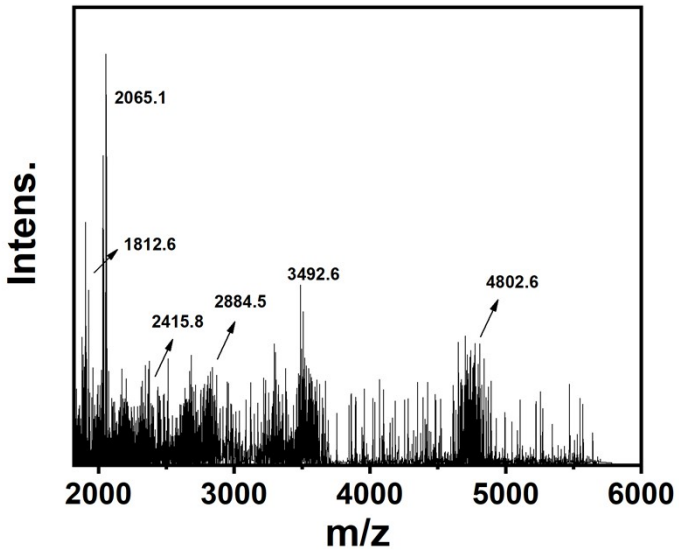

Figure S14. ESI-MS of **$Mo_{24}V_{30}P_{48}$**

Table S2. Assignment of peaks of **$Mo_{24}V_{30}P_{48}$**

Observed m/z	Calculated m/z	Charge □	Polyanion □
1812.6	1811.2	-8	$\{Na_{24}[(V^{V}O_2)_{30}(Mo^{VI}O_4)_{12}(PhPO_3)_{48}(CH_3COO)_{12}](CO_3)_2\}^{8-}$
2065.1	2063.8	-7	$\{Na_{25}[(V^{V}O_2)_{30}(Mo^{VI}O_4)_{12}(PhPO_3)_{48}(CH_3COO)_{12}](CO_3)_2\}^{7-}$
2415.8	2415.2	-6	$\{Na_{26}[(V^{V}O_2)_{30}(Mo^{VI}O_4)_{12}(PhPO_3)_{48}(CH_3COO)_{12}](CO_3)_2\}^{6-}$
2884.5	2885.4	-5	$\{Na_{27}[(V^{V}O_2)_{30}(Mo^{VI}O_4)_{12}(PhPO_3)_{48}(CH_3COO)_{12}](CO_3)_2\}^{5-}$
3492.6	3491.7	-4	$\{Na_{28}[(V^{V}O_2)_{30}(Mo^{VI}O_4)_{12}(PhPO_3)_{48}(CH_3COO)_{12}](CO_3)_2\}^{4-}$
4802.6	4803.4	-3	$\{Na_{29}[(V^{V}O_2)_{30}(Mo^{VI}O_4)_{12}(PhPO_3)_{48}(CH_3COO)_{12}](CO_3)_2\}^{3-}$

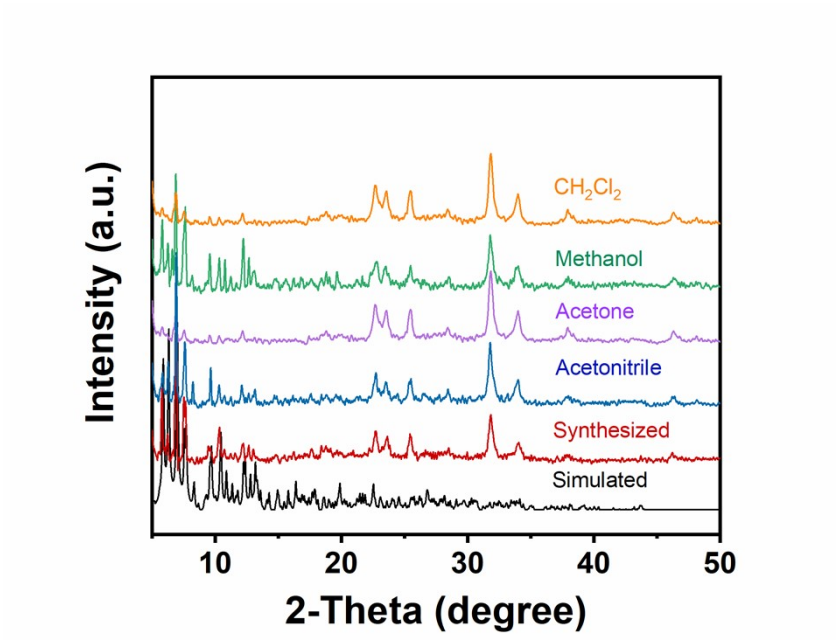

Figure S15. PXRD patterns of $\mathbf{Mo_{24}V_{30}P_{48}}$ in different solutions.

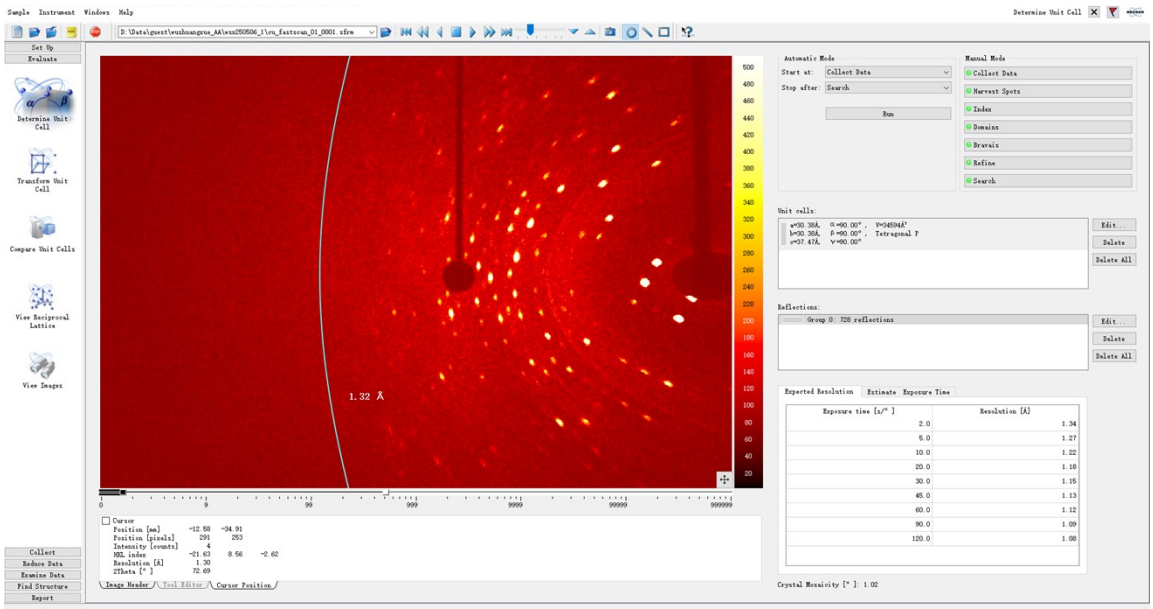

Figure S16. ESI-MS of $\mathbf{Mo_{24}V_{30}P_{48}}$

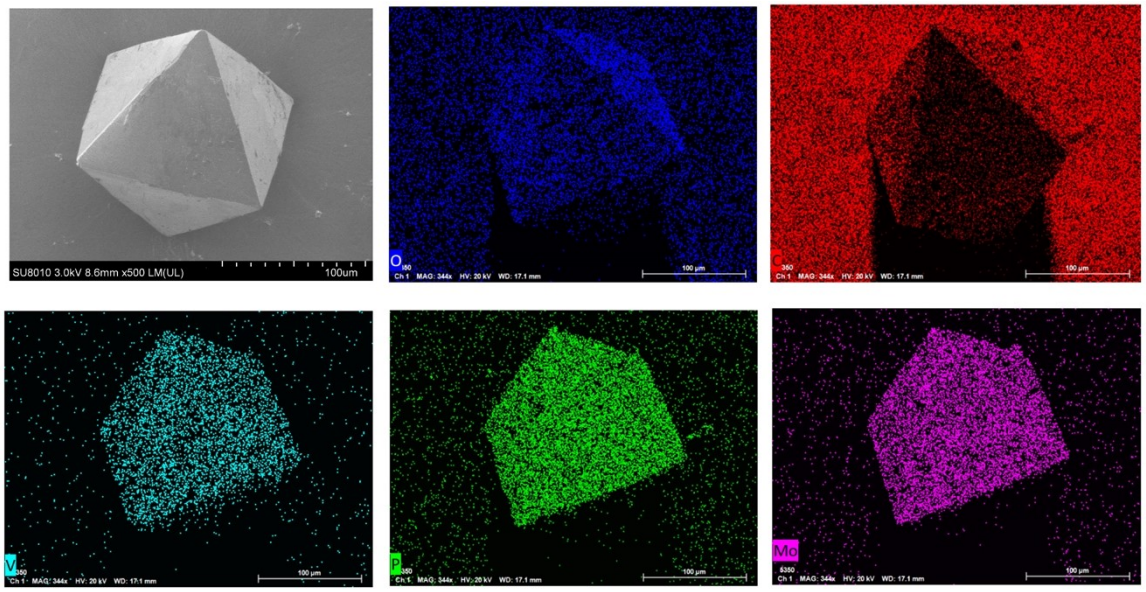

Figure S17. The SEM images and elemental mapping of $Mo_{24}V_{30}P_{48}$

Table S3. Catalytic testing of $Mo_{24}V_{30}P_{48}$ under various experimental conditions for 2-tert-butylphenol.

Entry	Cat. (mg)	H_2O_2 (μmol)	Solvent	Tem. (℃)	Covn. (%)	Sel. (%)
1	10	100	MeCN	80	97.6	98.4
2	10	100	MeOH	80	84.8	82.6
3	10	100	CH_2Cl_2	80	57.6	56.7
4	10	100	CH_3OCH_3	80	83.4	84.2
5	5	100	MeCN	80	66.7	97.7
6	0	100	MeCN	80	21.5	63.2
7	20	100	MeCN	80	99.6	98.9
8	10	0	MeCN	80	Trace	Trace
9	10	40	MeCN	80	52.3	66.4
10	10	80	MeCN	80	75.8	89.8

11	10	200	MeCN	80	98.3	99.5
12	10	100	MeCN	50	64.8	59.7

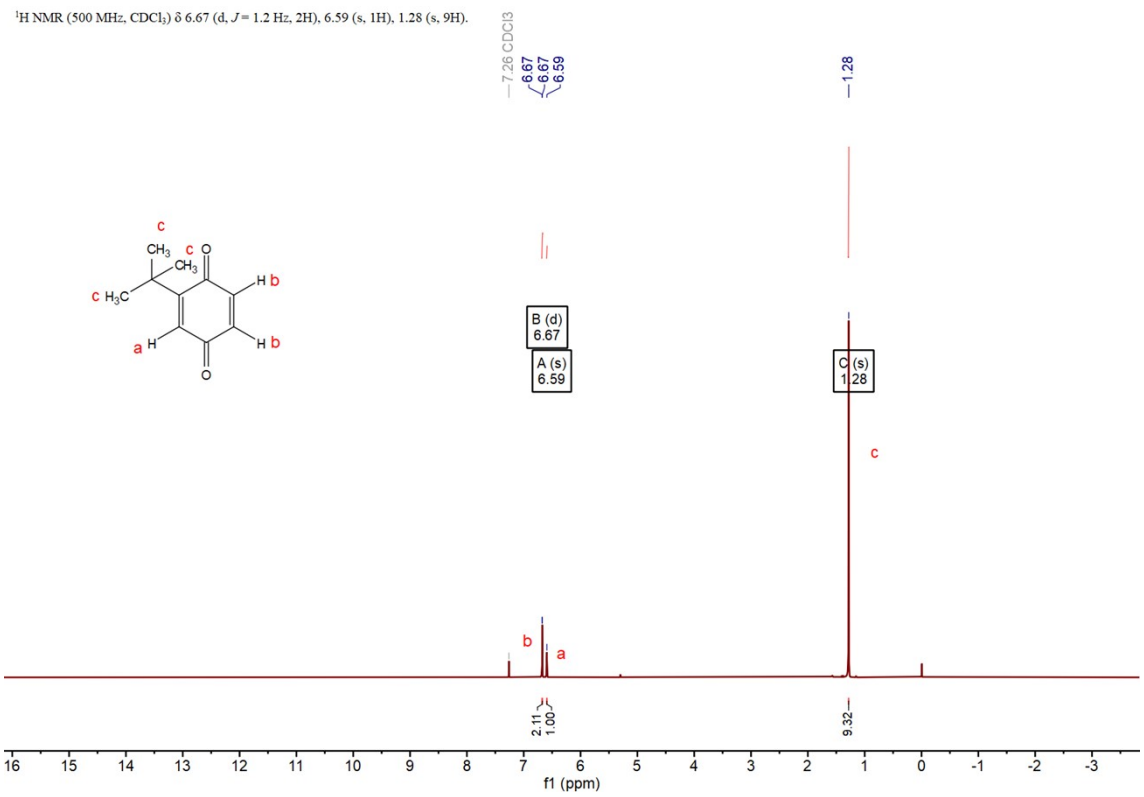

Figure S18. [1]HNMR of 2-tert-Butyl-1,4-benzoquinone

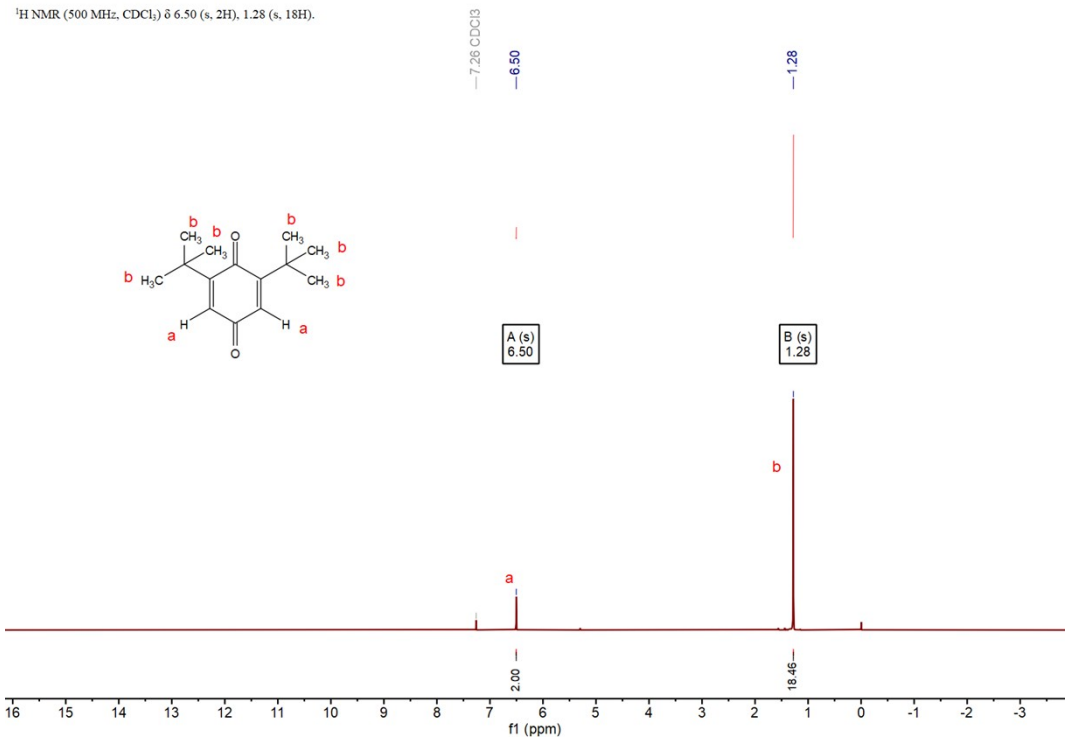

Figure S19. [1]HNMR of 2,6-Di-tert-Butyl-1,4- benzoquinone

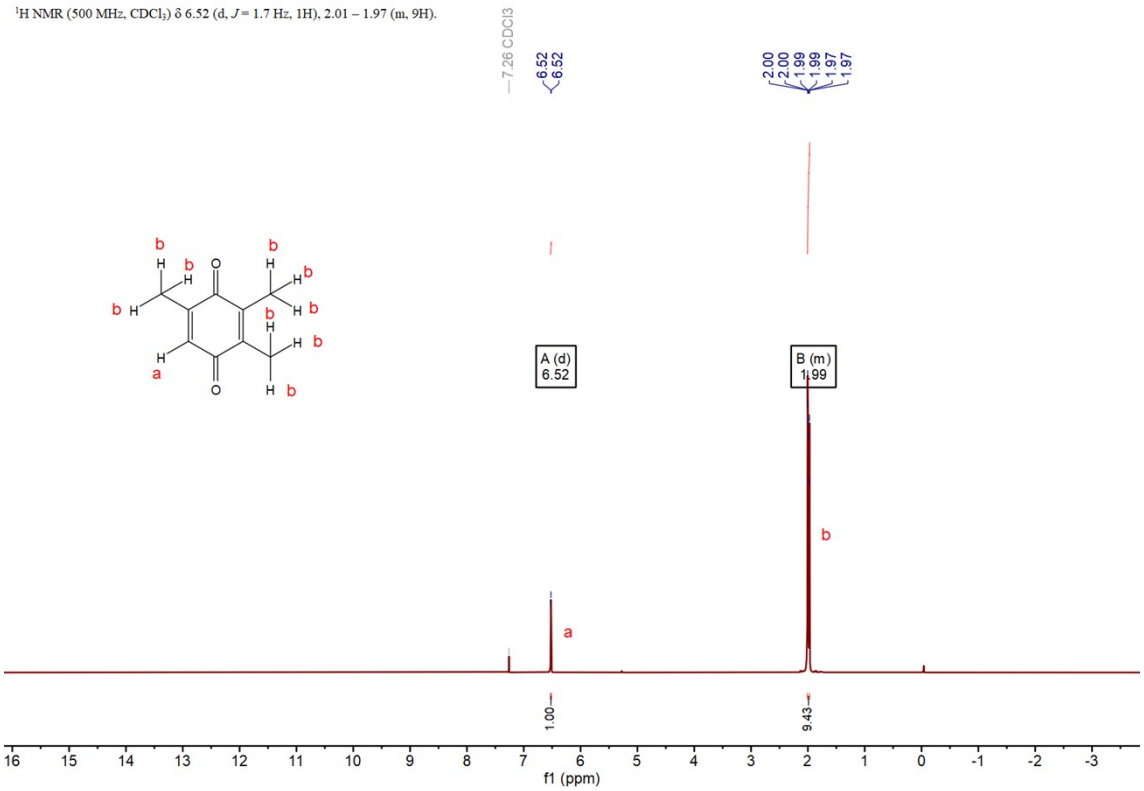

Figure S20. 1HNMR of 2,3,6-Trimethyl-1,4- benzoquinone

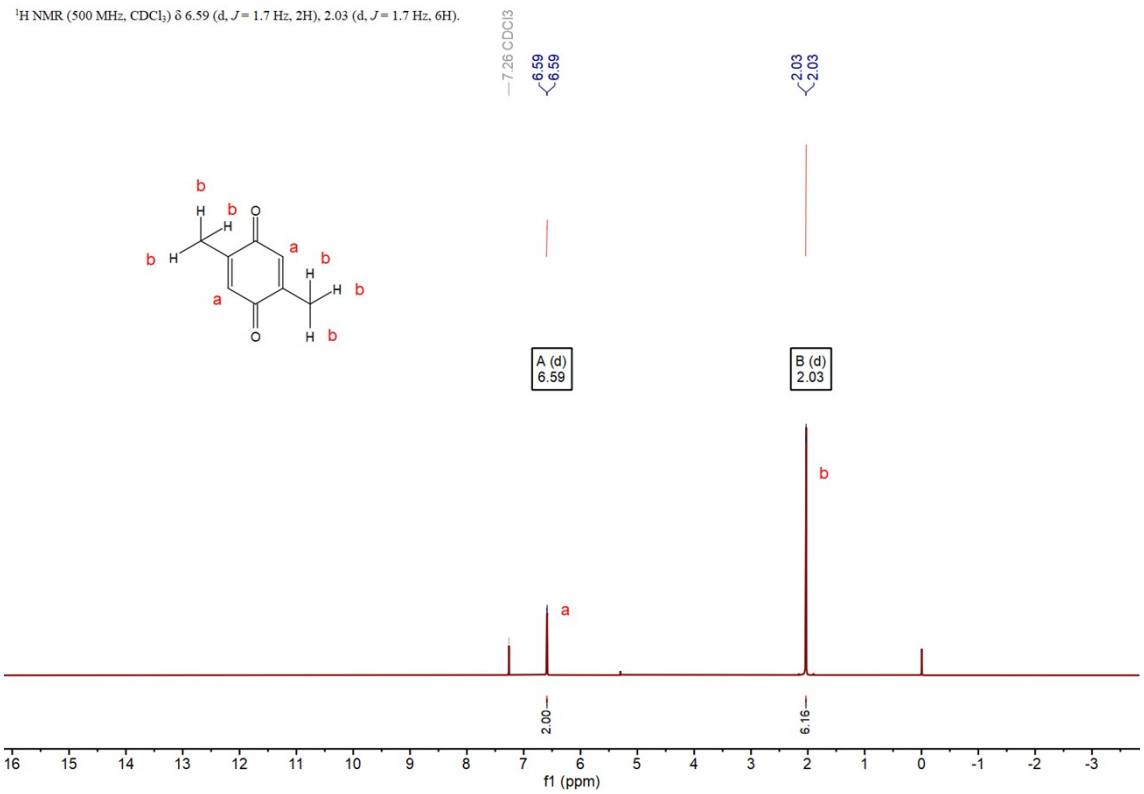

Figure S21. 1HNMR of 2,5-Dimethyl-1,4- benzoquinone

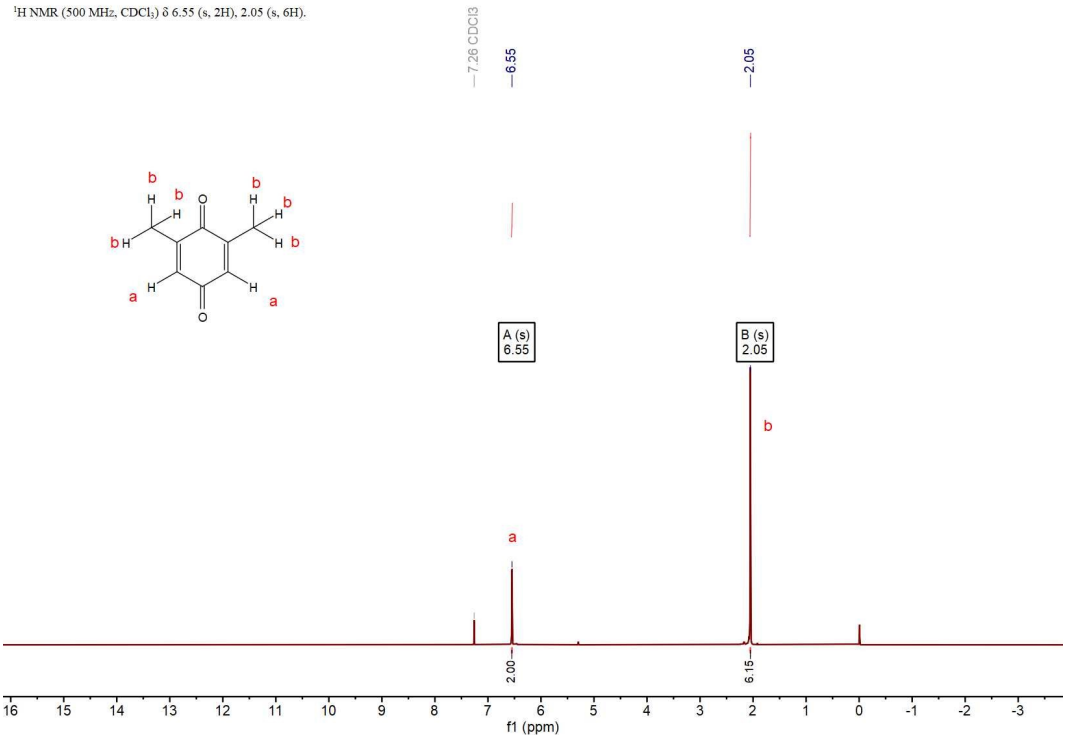

Figure S22. 1HNMR of 2,6-Dimethyl-1,4- benzoquinone

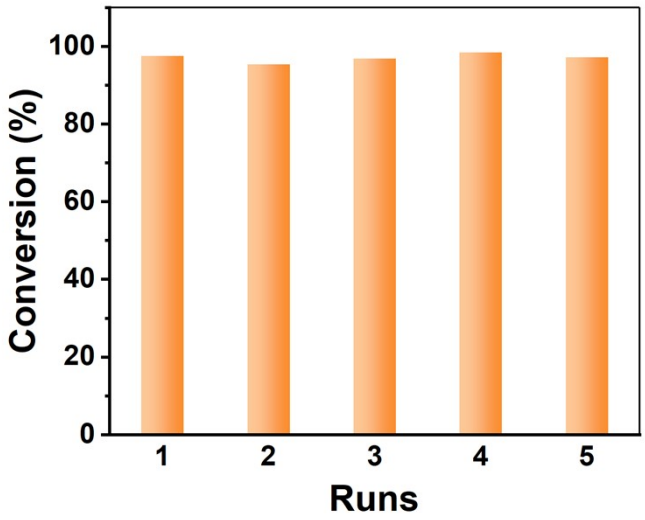

Figure S23. Recycling experiments for the oxidation of 2-tert-butylphenol with $Mo_{24}V_{30}P_{48}$

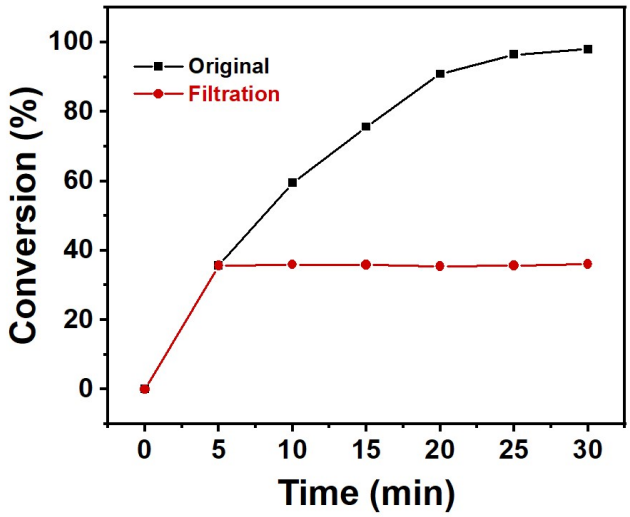

Figure S24. Conversion curve of 2-tert-butylphenol catalysed by $Mo_{24}V_{30}P_{48}$ (black), catalyst was ffltered out at 5 min of the reaction (red)

Table S4. Bond angles for $Mo_{24}V_{30}P_{48}$

Atom	Atom	Atom	Angle/°	Atom	Atom	Atom	Angle/°
O8	Mo1	O1	95.5(8)	Mo1	O8	Mo4	83.5(7)
O8	Mo1	O10	157.5(8)	Mo1	O8	V4	138.3(10)
O8	Mo1	O12	88.5(8)	Mo4	O8	V4	138.1(11)
O34	Mo2	O30	79.7(8)	P8	O10	Mo1	141.6(12)
O48	Mo2	O34	85.7(11)	P1	O12	Mo1	124.9(10)
O48	Mo2	O82	157.5(10)	C73	O16	Mo1	118.3(12)
O24	Mo3	O9	83.8(7)	P1	O18	V4	135.1(12)
O68	Mo3	O9	175.1(9)	P10	O20	Mo4	138.2(12)
O72	Mo3	O9	77.0(7)	P4	O22	V9	143.7(13)
O1	Mo4	O4	87.8(8)	C20	C19	C24	120

O1	Mo4	O20	156.3(8)	C21	C20	C19	120
O62	Mo4	O20	98.4(9)	C22	C21	C20	120
O48	Mo5	O40	81.5(8)	C23	C22	C21	120
O48	Mo5	O60	89.5(12)	C22	C23	C24	120
O94	Mo5	O84	99.0(11)	C19	C24	P2	120.1(5)
O24	Mo6	O26	97.3(9)	C23	C24	P2	119.9(5)
O24	Mo6	O32	156.2(8)	C23	C24	C19	120
O56	Mo6	O58	175.6(9)	Mo6	O24	Mo3	81.1(9)
O1	V1	O79	87.1(9)	V9	O24	Mo3	137.4(10)
O76	V1	O50	97.2(10)	V9	O24	Mo6	141.3(11)
O76	V1	O79	176.0(10)	P6	O28	Mo6	127.5(12)
$O7^{1}$	V2	$O86^{1}$	90.4(10)	P6	O28	Na4	138.7(13)
O99	V2	O100	91.0(12)	C77	O30	Mo2	117.6(14)
O99	V2	O13	172.3(15)	P7	O32	Mo6	140.0(15)
$O42^{2}$	V3	O59	93.3(13)	P2	O34	Mo2	127.2(16)
$O42^{2}$	V3	O92	84.1(12)	P1	O36	$V1^{1}$	140.5(11)
$O42^{2}$	V3	O11	91.0(11)	P6	O38	$V4^{2}$	147.0(14)
O8	V4	O15	87.5(9)	C77	O40	Mo5	115.7(15)
$O38^{1}$	V4	O8	173.1(10)	P3	O42	$V3^{1}$	146.6(15)
$O38^{1}$	V4	O15	87.6(9)	P8	O44	V1	139.5(16)
O26	V5	O98	87.7(10)	Mo2	O48	Mo5	82.0(10)
O80	V5	O26	170.4(11)	Mo2	O48	V8	139.2(15)
O17	V6	$O54^{3}$	86.7(8)	P9	O59	V3	144(2)
O17	V6	O54	86.7(8)	P11	O60	Mo5	142(2)
$O111^{2}$	V7	O5	92.8(9)	P11	O61	V8	144(2)
O111	V7	O5	92.8(9)	P12	O64	V9	141.5(15)
O45	V7	$O111^{3}$	87.2(9)	P10	O70	V4	140.2(16)
O2	V8	O48	93.7(11)	P3	O72	Mo3	125.2(13)
O2	V8	$O74^{1}$	94.5(12)	C48	C47	C46	120
O2	V8	O108	103.3(13)	C47	C48	C43	120
O22	V9	O41	92.0(10)	P5	O74	$V8^{2}$	144.7(17)
O24	V9	O22	172.0(9)	C50	C49	P8	119.7(5)
O24	V9	O41	88.3(10)	C50	C49	C54	120
O12	P1	C26	105.6(9)	Mo2	O78	Mo5	80.7(10)
O18	P1	C26	110.2(10)	V3	O78	Mo2	140.8(15)
O18	P1	O36	111.0(12)	V3	O78	Mo5	138.2(15)
O34	P2	C24	107.4(12)	P2	O80	V5	144.0(16)
O34	P2	O108	110.5(17)	P9	O82	Mo2	143.0(19)
O108	P2	C24	110.3(11)	P5	O84	Mo5	121.2(15)
O42	P3	O72	110.6(13)	O59	P9	O82	109.8(19)
O72	P3	C37	102.7(10)	O82	P9	C18	106.9(13)
O98	P3	O72	111.5(14)	O86	P9	C18	113.3(14)
O22	P4	O4	114.4(13)	O20	P10	C55	101.9(9)
O22	P4	O50	106.3(12)	O70	P10	O20	114.3(13)
O22	P4	C66	107.4(8)	O70	P10	O96	109.9(15)
O74	P5	O84	106.8(17)	O60	P11	O61	110(2)
O84	P5	C35	107.3(11)	O60	P11	C68	108.9(13)
O38	P6	O52	114.7(14)	O111	P11	C68	110.2(15)
O38	P6	C47	101.1(9)	O64	P12	C6	105.8(10)
O32	P7	C7	105.2(11)	O66	P12	O64	110.1(13)

O110	P7	O7	108.9(17)	O100	P12	O64	105.1(14)
O10	P8	C49	104.8(10)	Mo1	O1	V1	138.4(10)
O44	P8	O54	105.1(15)	Mo4	O1	Mo1	83.9(7)
O44	P8	C49	112.3(12)	Mo4	O1	V1	137.6(10)

[1]+Y,3/2-X,+Z; [2]3/2-Y,+X,+Z; [3]3/2-X,3/2-Y,+Z

Table S5. Bond lengths for $Mo_{24}V_{30}P_{48}$

Atom	Atom	Length/Å	Atom	Atom	Length/Å	Atom	Atom	Length/Å
Mo1	O1	1.966(19)	C1	C2	1.39	P1	O12	1.563(19)
Mo1	O8	1.948(19)	C1	C6	1.39	P1	O18	1.44(2)
Mo1	O10	2.03(2)	C2	C3	1.39	P1	C26	1.787(6)
Mo1	O12	2.052(17)	C3	C4	1.39	P1	O36	1.525(18)
Mo1	O14	1.718(18)	C4	C5	1.39	P2	C24	1.789(6)
Mo1	O16	2.236(16)	C5	C6	1.39	P2	O34	1.48(3)
Mo2	O30	2.297(18)	C7	C8	1.39	P2	O80	1.50(3)
Mo2	O34	2.09(3)	C7	C12	1.39	P2	O108	1.54(3)
Mo2	O48	1.96(3)	C8	C9	1.39	P3	C37	1.786(6)
Mo2	O78	2.01(3)	C9	C10	1.39	P3	O42	1.53(3)
Mo2	O82	2.09(3)	C10	C11	1.39	P3	O72	1.59(2)
Mo2	O90	1.73(2)	C11	C12	1.39	P3	O98	1.46(2)
Mo3	O24	2.04(2)	O6	C73	1.234(10)	P4	O4	1.533(19)
Mo3	O26	1.94(2)	O6	Na6	2.54(2)	P4	O22	1.45(2)
Mo3	O66	2.02(2)	O7	V2[2]	2.21(3)	P4	O50	1.53(2)
Mo3	O68	1.719(18)	O7	Na4	2.90(3)	P4	C66	1.784(6)
Mo3	O72	2.06(2)	O7	Na7	2.32(3)	P5	C35	1.785(6)
Mo3	O9	2.296(18)	O10	Na1[1]	2.51(2)	P5	O74	1.50(3)
Mo4	O1	1.949(18)	O12	Na1[1]	2.48(2)	P5	O84	1.57(3)
Mo4	O4	2.026(19)	O16	C73	1.245(9)	P5	O92	1.48(3)
Mo4	O6	2.281(15)	O16	Na1[1]	2.35(2)	P6	O28	1.53(2)
Mo4	O8	1.981(19)	O18	Na2[1]	2.61(2)	P6	O38	1.43(2)
Mo4	O20	2.04(2)	C13	C14	1.39	P6	O52	1.54(2)
Mo4	O62	1.669(19)	C13	C18	1.39	P6	C47	1.785(6)
Mo5	O40	2.293(18)	C14	C15	1.39	P6	Na2	3.193(18)
Mo5	O48	2.02(3)	C15	C16	1.39	P7	C7	1.782(6)
Mo5	O60	2.05(3)	C16	C17	1.39	P7	O7	1.53(3)
Mo5	O78	2.02(3)	C17	C18	1.39	P7	O32	1.54(3)
Mo5	O84	2.13(3)	O20	Na6	2.49(2)	P7	O110	1.51(3)
Mo5	O94	1.73(2)	C19	C20	1.39	P8	O10	1.54(2)
Mo6	O24	1.97(2)	C19	C24	1.39	P8	O54	1.51(3)
Mo6	O26	2.00(2)	C20	C21	1.39	P8	C49	1.785(6)
Mo6	O28	2.07(2)	C21	C22	1.39	P9	C18	1.786(6)
Mo6	O32	2.04(2)	C22	C23	1.39	P9	O59	1.48(3)
Mo6	O56	1.683(18)	C23	C24	1.39	P9	O82	1.47(3)
Mo6	O58	2.244(18)	C25	C26	1.39	P9	O86	1.45(3)
V1	O1	2.007(19)	C25	C30	1.39	P10	O20	1.56(2)
V1	O36[2]	1.928(18)	C26	C27	1.39	P10	O70	1.53(2)

V1	O44	1.95(3)	C27	C28	1.39	P10	O96	1.53(3)
V1	O50	1.98(2)	C28	C29	1.39	P10	C55	1.787(6)
V1	O76	1.92(2)	C29	C30	1.39	P11	O60	1.50(3)
V1	O79	2.11(3)	O28	Na4	2.58(3)	P11	O61	1.54(3)
V2	O7[1]	2.21(3)	O30	C77	1.246(10)	P11	O111	1.48(3)
V2	O86[1]	2.27(3)	O30	Na7	2.36(3)	P11	C68	1.789(6)
V2	O96	2.15(3)	O32	Na4	2.49(2)	P12	C6	1.787(6)
V2	O100	2.29(3)	C31	C32	1.39	P12	O64	1.57(2)
V2	O13	2.157(14)	C31	C36	1.39	P12	O66	1.53(2)
V2	O99	2.063(14)	C32	C33	1.39	P12	O100	1.47(3)
V3	O42[2]	1.88(3)	C33	C34	1.39	C50	C51	1.39
V3	O59	1.91(3)	C34	C35	1.39	C51	C52	1.39
V3	O78	1.95(3)	C35	C36	1.39	C52	C53	1.39
V3	O92	1.97(3)	O34	Na7	2.57(3)	C53	C54	1.39
V3	O11	2.005(16)	C37	C38	1.39	O80	Na8[1]	2.59(3)
V3	O37	2.012(17)	C37	C42	1.39	O82	Na7	2.61(3)
V4	O8	2.01(2)	C38	C39	1.39	O84	Na3	2.45(3)
V4	O15	2.22(3)	C39	C40	1.39	O86	V2[2]	2.27(3)
V4	O18	2.02(2)	C40	C41	1.39	O86	Na5	2.32(3)
V4	O38[1]	1.96(2)	C41	C42	1.39	O92	Na8	2.65(3)
V4	O70	1.89(2)	O36	V1[1]	1.928(18)	O96	Na4[1]	2.31(3)
V4	O88	1.94(2)	O36	Na2[1]	2.64(2)	O98	Na8[1]	2.49(3)
V5	O21	2.25(3)	O38	V4[2]	1.96(2)	O100	Na6	2.30(3)
V5	O26	2.01(3)	O38	Na2	2.61(2)	O108	Na8[1]	2.81(3)
V5	O63	1.95(2)	O40	C77	1.248(10)	O110	Na7	2.69(3)
V5	O80	1.95(3)	O40	Na3	2.40(3)	O111	Na3[1]	2.40(4)
V5	O98	2.01(2)	O42	V3[1]	1.88(3)	O111	Na3	2.97(4)
V5	O110	1.89(3)	O42	Na8[1]	2.60(3)	C55	C56	1.39
V6	O54	2.21(3)	V7	O111	2.22(4)	V8	O108	1.93(3)
V6	O54[1]	2.21(3)	V7	O111[3]	2.22(4)	V8	O3	2.241(17)
V6	O54[2]	2.21(3)	V7	O5	2.28(7)	V9	O22	2.01(2)
V6	O54[3]	2.21(3)	V7	O45	2.12(2)	V9	O24	1.91(2)
V6	O228	2.21(2)	V8	O2	1.74(2)	V9	O41	2.23(2)
V6	O17	2.03(2)	V8	O48	1.99(3)	V9	O52	1.95(2)
V7	O111[2]	2.22(4)	V8	O61	1.87(4)	V9	O64	1.84(2)
V7	O111[1]	2.22(4)	V8	O74[1]	1.93(3)	V9	O102	2.07(2)

[1]+Y,3/2-X,+Z; [2]3/2-Y,+X,+Z; [3]3/2-X,3/2-Y,+Z

Table S6. Comparison with other systems for 2,3,6-trimethylphenol oxidation

Catalyst	Oxidant	Temp. (°C)	Time (min)	Conv. (%)	Sel. (%)	Reference
$Mo_{24}V_{30}P_{48}$	H_2O_2	80	10	>99	>99	This work
γ-$PW_{10}V_2$	H_2O_2	80	4	>99	>99	3
$PW_{11}Ti$	H_2O_2	80	30	90	45	4
$PW_{11}Zr$	H_2O_2	80	60	90	30	5

V_2-POM/N-CNTs	H_2O_2	60	15	>99	>99	6
L-Mo_{132}	^{t}BuOOH	80	120	97	71	7
K-Mo_{132}	^{t}BuOOH	80	120	44	79	7
$[Cu(Htza)_2(H_2O)_2][BW_{12}O_{40}]\cdot 6H_2O$	^{t}BuOOH	60	8	>99	>99	8
$(Htza)_2(H_2O)]_3[SiW_{12}O_{44}]\cdot 14H_2O$	^{t}BuOOH	60	6	>99	>99	8
$H_3[CuI_3(L)_3]_2[PMo_{12}O_{40}]\cdot 4H_2O$	H_2O_2	80	5	>99	>99	9
$H[CuII_3(L)_3(OH)(HL)(H_2O)][PMo_{12}O_{40}]\cdot 5H_2O$	H_2O_2	80	8	>99	>99	9
$H_3[CuI_3(L)_3]_2[PW_{12}O_{40}]\cdot 6H_2O$	H_2O_2	80	6	>99	>99	9

References

1. G. M. Sheldrick, SADABS, Program for area detector adsorption correction; institute for inorganic chemistry, University of Göttingen, Germany, 2003.

2. O. V. Dolomanov, L. J. Bourhis, R. J. Gildea and J. A. K. Howard, Puschmann, H. OLEX2: a complete structure solution, refinement and analysis program, *J. Appl. Crystallogr.,* 2009, **42**, 339.

3. I. D. Ivanchikova, N. V. Maksimchuk, R. I. Maksimovskaya, G. M. Maksimov and O. N. Kholdeeva, Highly Selective Oxidation of Alkylphenols to p-Benzoquinones with Aqueous Hydrogen Peroxide Catalyzed by Divanadium-Substituted Polyoxotungstates, *ACS Catal*., 2014, **4**, 2706–2713.

4. O. A. Kholdeeva, T. A. Trubitsina and G. M. Maksimov, Synthesis, Characterization, and Reactivity of Ti(IV)-Monosubstituted Keggin Polyoxometalates, *Inorg. Chem.*, 2005, **44**, 1635–1642.

5. O. A. Kholdeeva, G. M. Maksimov and R. I. Maksimovskaya, Zr^{IV}-MonosubstitutedKeggin-Type Dimeric Polyoxometalates: Synthesis, Characterization, Catalysis of H_2O_2-BasedOxidations, and Theoretical Study, *Inorg. Chem*., 2006, **45**, 7224–7234.

6. V. Y. Evtushok, A. N. Suboch, O. Y. Podyacheva, Highly Efficient Catalysts Based onDivanadium-Substituted Polyoxometalate and N-Doped Carbon Nanotubes for SelectiveOxidation of Alkylphenols, *ACS. Catal*., 2018, **8**, 1297–1307.

7. J. Liu, N. Jiang, J. M. Lin, Z. B. Mei, L. Z. Dong, Y. Kuang, J. J. Liu, S. J. Yao, S. L. Li and Y. Q. Lan, Structural Evolution of Giant Polyoxometalate: From “Keplerate” to “Lantern” Type Mo_{132} for Improved Oxidation Catalysis, *Angew. Chem. Int. Ed.,* 2023, **62**, e202304728.

8. S. Chang, Y. Chen and H. An, Polyoxometalate-based supramolecular porous frameworkswith dual-active centers towards highly efficient synthesis of functionalized p-benzoquinones, *Green Chem*., 2021, **23**, 8591–8602.

9. S. Chang, Y. Chen and H. An, Highly Efficient Synthesis of p-Benzoquinones Catalyzed byRobust Two-Dimensional POM-Based Coordination Polymers, *ACS Appl. Mater. Inter*., 2021, **13**, 21261–21271.